
Graph-Constrained Structure Search for Tensor Network Representation

Anonymous Author(s)

Affiliation

Address

email

Abstract

1 Recent works paid effort on the structure search issue for tensor network (TN)
2 representation, of which the aim is to select the optimal network for TN contraction
3 to fit a tensor. In practice, however, it is more inclined to solve its sub-problem:
4 searching TN structures from candidates with a similar topology like a cycle or lat-
5 tice. We name this problem *the graph-constrained structure search*, and it remains
6 open to this date. In this work, we conduct a thorough investigation of this issue
7 from both the theoretical and practical aspects. Theoretically, we prove that the
8 TN structures are generally irregular under graph constraints yet can be universally
9 embedded into a low-dimensional regular discrete space. Guided by the theoretical
10 results, we propose a simple algorithm, which can encode the graph-constrained
11 TN structures into fixed-length strings for practical purposes by a “random-key”
12 trick, and empirical results demonstrate the effectiveness and efficiency of the
13 proposed coding method on extensive benchmark TN representation tasks.

14 1 Introduction

15 Tensor networks (TNs) are recognized as a popular framework for solving extremely
16 high-dimensional problems arising in domains such as quantum simulation, machine
17 learning and signal processing. In general, TNs are used to represent the high-
18 dimensional states/models/data by a network of low-dimensional tensors (*a.k.a.*, cores),
19 such that the requirement on computation and storage would be significantly reduced.
20

21 It is of importance to select an appropriate structure in the practical
22 use of TNs. There are many studies on learning TN ranks for specific
23 models [26–28, 43, 46, 47] to name a few, and recently several works
24 paid the effort on learning more general TN structures with arbitrary
25 topology [17, 19, 21, 25]. Surprisingly, however, none of them can
26 effectively solve a seemingly easier task: *how to learn the optimal matching*
27 *from the modes onto the cores of a TN?* For instance as illustrated in
28 Figure 1, there are three different candidates to represent a tensor
29 ring (TR) [47]. We need algorithms, which can learn the optimal
30 one from the three. It is actually a special case of learning the optimal
31 TN structures under *graph constraints*, a sub-problem of the existing
32 structure search for TN representation.

33 The state of affairs raises important unresolved questions. *Is the afore-*
34 *mentioned task really easier than the general structure search? What*
35 *are the properties of TN structures under graph constraints, and how to*
36 *effectively solve the problem in practice?*

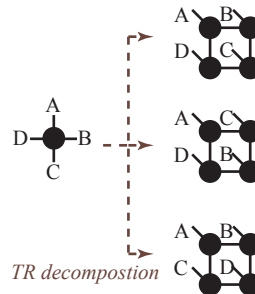


Figure 1: Which tensor ring (TR) is the optimal?

37 In this work, we shed light on these questions through a theoretical and empirical investigation of the
 38 graph-constrained TN structures.

39 We first prove the graph constraint makes TN structures being irregular. In particular, both the
 40 addition and random perturbation is not closed on the candidate set. This result helps to explain
 41 why the conventional search algorithms on grids give no guarantee of feasibility of the solutions.
 42 Furthermore, on the scale of the search problem, we prove the *symmetry* of the graph-constraint plays
 43 a role to determine the cardinality of TN structures, yet there exists a universal cardinality bound
 44 across a varies of practical TNs, such as tensor train (TT) [30], tensor ring (TR) and PEPS [38]. The
 45 result reveals the possibility to construct a regular discrete space, from which we can represent those
 46 irregular TN structures by elements in a compact manner.

47 Guided by the theoretical results, this work also sheds light on a practical solution for the graph-
 48 constrained structure search issue. We propose a novel coding method to encode TN structures into
 49 fix-length strings by a “random-key” trick, a random mapping from TN structure space to coding
 50 space. The regularity of the coding space allows to apply the population-based algorithms equipped
 51 with the proposed coding method to tackling the search issue for TN representation effectively. We
 52 conduct extensive experimentation on a variety of benchmarks. The results show that the proposed
 53 method often obtain better TN structures than many existing rank-selection and structure search
 54 algorithms.

55 2 Preliminaries and problem setup

56 In this section, we present the basic concepts on tensor network (TN), and give a formal definition of
 57 the *graph-constrained* structure search for TN representation.

58 2.1 Tensor network (TN) and structure search for tensor network representation (TNR)

59 An order- N tensor is a multi-dimensional array of real numbers represented by $\mathcal{X}_{i_1, i_2, \dots, i_N} \in$
 60 $\mathbb{R}^{I_1 \times I_2 \times \dots \times I_N}$, where $i_m, m \in [N]$ is defined as the *index* regarding the m th mode of \mathcal{X} ¹ and $[N]$
 61 denotes a set of integers from 1 to N . *Tensor contraction* [10], a binary operation on tensors, is
 62 defined as a multiplication of two tensors under their same indices. For instance, given two order-2
 63 tensors $\mathcal{A}_{i,j} \in \mathbb{R}^{I \times J}$, $\mathcal{B}_{j,k} \in \mathbb{R}^{J \times K}$, the tensor contraction of \mathcal{A} and \mathcal{B} under the index j returns
 64 $\mathcal{C}_{i,k} = \mathcal{A}_{i,j} \mathcal{B}_{j,k} \in \mathbb{R}^{I \times K}$, which is equivalent to the matrix multiplication.

65 A *tensor network (TN)* is roughly defined as a collection of tensors (*a.k.a.*, cores), which are
 66 tensor-contracted under some, or all, of their indices according to a specific pattern [29]. Recent
 67 works [25, 42] show that the “patterns” of TNs can be precisely described by edge-weighted simple
 68 graphs. TN structures thus can be formulated by adjacency matrices of graphs. Formally, we define
 69 the TN with a general “pattern” as follows.

70 **Definition 1 (Tensor network.)** Let $\mathbb{A}_R = \left\{ \mathbf{A} \in (\mathbb{Z}_{R+1})^{N \times N} \mid \mathbf{A}(i, i) = 0, \forall i \in [N], \text{ and } \mathbf{A} = \mathbf{A}^\top \right\}$,
 71 an order- N tensor network (TN) of the size $I_1 \times I_2 \times \dots \times I_N$ under a structure $\mathbf{A} \in \mathbb{A}_R$ defines a
 72 mapping :

$$\mathcal{X} = TN(\mathbb{V}; \mathbf{A}) \in \mathbb{R}^{I_1 \times I_2 \times \dots \times I_N}, \quad (1)$$

73 where $\mathbb{V} = \{\mathcal{V}_i, i \in [N]\}$ represents a collection of cores in which the size of $\mathcal{V}_i, i \in [N]$ equals
 74 the multiplication of I_i and all non-zero entries of $\mathbf{A}(i, \cdot)$, and $TN(\cdot; \mathbf{A})$ denotes a series of tensor
 75 contractions of \mathbb{V} under the indices [25] described by \mathbf{A} .

76 We observe that Definition. 1 models a rich family of TNs with the ranks upper-bounded by R (due
 77 to \mathbb{Z}_{R+1}), including TT, TR, PEPS and *etc.*, but also note that the TNs that contain internal cores are
 78 not included in this form.

79 Tensor network representation (TNR) of a tensor \mathcal{X} is defined as finding a specific core-set \mathbb{V} such
 80 that Eq. (1) holds. The *structure search for TNR* is thus to find the optimal matrix $\mathbf{A} \in \mathbb{A}_R$, such that
 81 \mathcal{X} can be represented by \mathbb{V} that satisfies Eq. (1). In particular, the search problem can be solved by

$$\min_{\mathbf{A} \in \mathbb{A}_R} \phi_{\mathcal{X}}(\mathbf{A}), \quad \text{s.t. } \mathcal{X} = TN(\mathbb{V}; \mathbf{A}) \text{ for some } \mathbb{V}, \quad (2)$$

¹The indices would be omitted for brevity if there is no confusion.

82 where $\phi_{\mathcal{X}} : \mathbb{A}_R \rightarrow \mathbb{R}$ denotes a measure of the TN structures like compression ratio. Note that
 83 similar frameworks were also introduced in works [17, 21], where the entries of \mathbf{A} corresponds to
 84 the TN-ranks formulated as a vector in those works. Lemma 5 in Sec. 3 will show the matrix form of
 85 \mathbf{A} would provide additional structural information to analyse the property of TN structures.

86 2.2 Graph-constrained structure search for TNR

87 The graph-constrained structure search issue is also modeled as (2) yet constraining the feasible space
 88 \mathbb{A}_R into a graph-induced subset, in which the TN structures have similar topological forms. To build
 89 the connection to graphs, we first show the existence of a bijective mapping from \mathbb{A}_R to a graph
 90 space.

91 **Lemma 2** *There is a bijective mapping $\Psi : \mathbb{A}_R \rightarrow \mathbb{G}_R$, where \mathbb{G}_R denotes a set containing all
 92 possible vertex-labeled, simple yet weighted graphs $(G, f_R) = (V, E, f_R)$ with N vertices and a
 93 edge-weighting function $f_R : e \in E \rightarrow [R]$, and we name the unweighted part G the topology of TN
 94 a TN structure.*

95 The claim is naturally true by the relation between graphs and the adjacency matrices. The bijection
 96 in Lemma 2 implies that for each $\mathbf{A} \in \mathbb{A}_R$ we can always find a unique (G, f_R) corresponding to
 97 it. Table 1 in the *supplementary material* illustrates the correspondence between graphs and the
 98 well-known TNs. We next construct graph-constrained TN structures by the isomorphism of a graph
 99 $G_0 = (V, E_0)$ and the mapping Ψ given in Lemma 2. A formal definition is given as follow.

100 **Definition 3 (Graph-constrained TN structures.)** *Given a vertex-labeled simple graph $G_0 =$
 101 (V, E_0) and the mapping Ψ in Lemma 2, the TN structures under G_0 are defined as*

$$\mathbb{H}_{G_0, R} = \{\mathbf{H} \in \mathbb{A}_R \mid G_{\mathbf{H}} \cong G_0 \text{ where } (G_{\mathbf{H}}, f_{R, \mathbf{H}}) = \Psi(\mathbf{H})\}, \quad (3)$$

102 where \cong denotes the graph isomorphism.

103 As given in Definition 3, $\mathbb{H}_{G_0, R}$ is a subset of \mathbb{A}_R and its elements own the topologies being
 104 isomorphic to G_0 . For instance, suppose G_0 to be a cycle graph of 4 vertices, *i.e.*, C_4 , then $\mathbb{H}_{C_4, R}$
 105 contains all TR structures of order-4 with the ranks upper-bounded by R as Figure 1. It is thus
 106 expected to solve the mentioned optimal matching problem by searching structures on $\mathbb{H}_{G_0, R}$. Not
 107 only that, but also note $\mathbb{H}_{G_0, R}$ equals \mathbb{A}_R if G_0 is a completion graph, *i.e.*, K_N . Next, we define the
 108 problem of graph-constrained structure search for TNR by $\mathbb{H}_{G_0, R}$.

109 **Definition 4 (Graph-constrained structure search for TNR.)** *Given a graph G_0 and the corre-
 110 sponding $\mathbb{H}_{G_0, R}$ obtained as Definition 3, the graph-constrained structure search for TNR is to solve
 111 the following problem:*

$$\min_{\mathbf{H} \in \mathbb{H}_{G_0, R}} \phi_{\mathcal{X}}(\mathbf{H}), \quad \text{s.t. } \mathcal{X} = TN(\mathbb{V}; \mathbf{H}) \text{ for some } \mathbb{V}. \quad (4)$$

112 It is shown from Definition 4 that the set $\mathbb{H}_{G_0, R}$ restricts the optimization process only searching on
 113 the TN structures, which has the same topology G_0 up to *permutations of the vertices* [5]. Moreover,
 114 although (4) owns a similar form to its unconstrained counterpart (2), it will be proved in the next
 115 section that the existing algorithms on (2) may be not available on the graph-constrained search issue.

116 **Remark.** Note that Definition 1 allows the entries of \mathbf{A} to equal 1, which implies the rank-one
 117 contraction between cores. According to the fact given in [25, 42] that the weight-one edges can
 118 be removed from TNs, we thus know that the solution of (4) would have a *subgraph* of G_0 as its
 119 “true” topology. Therefore, solving (4) has the capability of achieving not only isomorphic but also
 120 subgraphs of G_0 .

121 3 Algebraic properties of graph-constrained TN structures

122 In this section, we focus on the properties of $\mathbb{H}_{G_0, R}$, the set containing all TN structures constrained
 123 under a graph G_0 . From an algebraic perspective, we first show $\mathbb{H}_{G_0, R}$ is irregular under most of
 124 graph constraints by proving that the set is not closed under addition and random perturbation. After
 125 that, we analyse the cardinality of $\mathbb{H}_{G_0, R}$, which reflects the scale of the search problem. We derive

126 the precise cardinality of $\mathbb{H}_{G_0,R}$ across many well-known TNs, and prove a universal cardinality
 127 bound of $\mathbb{H}_{G_0,R}$ under all connected low-degree graphs.

128 To understand the property of $\mathbb{H}_{G_0,R}$, we first prove all its elements own a factorization of the
 129 multiplication of a rank-induced matrix and a permutation matrix.

130 **Lemma 5 (Factorization of $\mathbb{H}_{G_0,R}$.)** *Given a vertex-labeled simple graph $G_0 = (V, E_0)$, for any
 131 $\mathbf{H} \in \mathbb{H}_{G_0,R}$, there exists a permutation matrix \mathbf{P} of the size $|V| \times |V|$ and a bijective linear mapping
 132 $\Omega_{G_0} : (\mathbb{Z}_{R+1})^{|E_0|} \rightarrow (\mathbb{Z}_{R+1})^{|V| \times |V|}$ such that \mathbf{H} can be factorized as*

$$\mathbf{H} = \mathbf{P}\Omega_{G_0}(\mathbf{r})\mathbf{P}^\top, \quad (5)$$

133 where $|\cdot|$ denotes the cardinality and $\mathbf{r} \in (\mathbb{Z}_{R+1})^{|E_0|}$ denotes the rank vector of dimension $|E_0|$.

134 Intuitively, Lemma 5 implies that the rank-induced matrix $\Omega_{G_0}(\mathbf{r})$ forms a linear sub-space of
 135 dimension $|E_0|$, then $\mathbb{H}_{G_0,R}$ takes all “flips and rotations” of the subspace into account due to the
 136 permutation matrix \mathbf{P} . A visual illustration of $\mathbb{H}_{G_0,R}$ is shown on the most left of Figure 2. We can
 137 see that $\mathbb{H}_{G_0,R}$ has an “irregular shape” visually, and this property is formally proved as follows.

138 **Proposition 6 (Irregularity of $\mathbb{H}_{G_0,R}$.)** *Assuming $R \geq 2$, the following two claims are held.*

- 139 1. *Addition (modulo $R + 1$) is not closed on $\mathbb{H}_{G_0,R}$ if $G_0 = (V, E_0)$ or its complement is not
 140 complete;*
- 141 2. *With a relatively sparse graph G_0 , the Bernoulli-distributed perturbation on $\mathbb{H}_{G_0,R}$ is not
 142 closed with a probability approximately being larger than $(1 - 1/R)^{|E_0|}$.*

143 The proof is given as *supplementary material*. Proposition 6 effectively say that the operations used
 144 in common search algorithms, such as the recombination and mutation in genetic algorithms (GAs)
 145 or progressive search in greedy methods, cannot guarantee the outputs being contained by $\mathbb{H}_{G_0,R}$,
 146 leading to the invalidation of those algorithms on this issue.

147 Next, we jump to the cardinality of $\mathbb{H}_{G_0,R}$, which reflects how many candidates we have under a
 148 graph constraint. From a information-theoretic perspective, the cardinality is proportional to the least
 149 required code length on TN structures in general. A smaller cardinality generally implies a easier
 150 search process especially for the population-based algorithms. Below, we first prove the cardinality
 151 of $\mathbb{H}_{G_0,R}$ under a general graph constraint.

152 **Lemma 7 (Cardinality of $\mathbb{H}_{G_0,R}$.)** *Given a vertex-labelled simple graph $G_0 = (V, E_0)$, we have*

$$\log(|\mathbb{H}_{G_0,R}|) = |E_0| \log(R) + \log(|V|!) - \log(|Aut(G_0)|), \quad (6)$$

153 where $\log(\cdot)$ denotes the natural logarithm and $Aut(G_0)$ denotes the graph automorphisms of G_0 .

154 As shown on the right of Eq. (6), the first two terms correspond to the TN-ranks and permutations as
 155 Lemma 5, respectively, while the third term $\log(|Aut(G_0)|)$ reflects the *symmetry* of G_0 . it implies
 156 the cardinality of $\mathbb{H}_{G_0,R}$ would be small if G_0 owns strong symmetry. From the TN perspective, it
 157 means the TNs with symmetric topologies like TR and the complete TN (CTN) [48] are expected to
 158 own a smaller size of $\mathbb{H}_{G_0,R}$. For those well-known TNs, we show their corresponding cardinality of
 159 $\mathbb{H}_{G_0,R}$ as follow.

160 **Proposition 8** *Assume order- N TN models, of which the ranks are upper-bounded by R , then we
 161 have*

- 162 1. **TT** [30]: $\log(|\mathbb{H}_{P_N,R}|) = (N - 1) \log(R) + \log(N!) - \log(2)$
- 163 2. **TR** [47]: $\log(|\mathbb{H}_{C_N,R}|) = N \log(R) + \log((N - 1)!) - \log(2)$
- 164 3. **CTN** [48]: $\log(|\mathbb{H}_{K_N,R}|) = (N^2 - N) \log(R)/2$
- 165 4. **T-tree** [42]: $(N - 1) \log(R) + \log(N) \leq \log(|\mathbb{H}_{T_N,R}|) \leq \log(|\mathbb{H}_{P_N,R}|)$
- 166 5. **PEPS** [38]: $\log(|\mathbb{H}_{L_{m,n}}|) \leq (2mn - m - n) \log(R) + \log((mn)!) - \log(4)$
- 167 6. **Tucker²** [36]: $\log(|\mathbb{H}_{K_{1,N}}|) = N \log(R)$

²Note that the Tucker model is not strictly contained by Definition. 1.

168 In Proposition 8, the inequalities for the T-tree models is due to the variety of the tree structures, and
 169 in PEPS the equality is held if m and n are relatively prime. We observe from Proposition 8 that
 170 TR would have a smaller $\mathbb{H}_{G_0,R}$ than TT in the case of large N . It is intuitively true since the TR
 171 structure is more symmetric than the one of TT. However, we also observe that, except CTN and the
 172 Tucker model, there always exists a factorial of N in the equations for the rest of TNs. It implies that
 173 the cardinality of $\mathbb{H}_{G_0,R}$ for those TNs is *not significantly different from each other*. Below, we prove
 174 the fact is true for all TNs, of which the corresponding G_0 is connected and low-degree.

175 **Proposition 9 (A universal cardinality bound on $\mathbb{H}_{G_0,R}$.)** Assume $G_0 = (V, E_0)$ is connected
 176 graph and its maximum degree Δ_{G_0} is a constant that is far less than $|V|$, then we have

$$\log(|\mathbb{H}_{G_0,R}|) \geq \mathcal{O}(|V| \log(R) + |V| \log(|V|)), \quad (7)$$

177 where $\mathcal{O}(\cdot)$ denotes the big- \mathcal{O} notation.

178 The result is proved by bounding the both $|E_0|$ and $|Aut(G_0)|$ in Lemma 5 by the maximum degree
 179 Δ_{G_0} using the Handshaking lemma known in graph theory and Theorem 2 given in [22], respectively.
 180 In addition, we also use the Stirling’s approximation [32] to obtain a tight bound for the logarithm of
 181 factorials to further simplify the expression.

182 The assumption of a small Δ_{G_0} is reasonable since in the practical TNs the cores are expected to be
 183 low-order (see Table 1 given in the supplementary material for instance). Proposition 9 means that
 184 there is a G_0 -independent bound on the cardinality of $\mathbb{H}_{G_0,R}$ for all connected and low-degree graphs,
 185 and we can see the bound is relatively tight by intuitively comparing the results with Proposition 8.

186 As shown in (7), the first term $|V| \log(R)$ corresponds to the number of all possible ranks bounded by
 187 R , and the second term $|V| \log(|V|)$ has the same scale to $\log(|V|!)$ for the Stirling’s approximation.
 188 It implies that, in the case of connected and low-degree G_0 , the cardinality of $\mathbb{H}_{G_0,R}$ is close to the
 189 combination of all possible $\Omega_{G_0}(\mathbf{r})$ and \mathbf{P} in Lemma 5. In other words, *the factorization given in*
 190 *Lemma 5 is nearly unique on $\mathbb{H}_{G_0,R}$* . From a pragmatic perspective, the result say that we can solve
 191 the constrained structure search issue from the factorization space as a alternative. More importantly,
 192 such the factorization space is independent to topology, because G_0 only determine the mapping Ω_{G_0} ,
 193 which is bijective, linear and fixed beforehand. The result guides us to find the practical solution on
 194 the graph-constrained structure search issue from the factorization space.

195 4 Encoding graph-constrained TN structures via a random-key trick

196 Inspired by the theoretical results, we introduce a practical coding method to embed the irregular TN
 197 structures into a regular discrete space, in which the population-based metaheuristics like GAs can be
 198 directly used for structure search. Last, experiments on a variety of benchmarks are implemented to
 199 demonstrate the effectiveness of the method.

200 4.1 Method

201 Figure. 2 depicts the coding process. We encode the elements of $\mathbb{H}_{G_0,R}$ from two ingredients: the
 202 rank-induced matrix $\Omega_{G_0}(\mathbf{r})$ and the permutation \mathbf{P} as Lemma 5. For the former, since the mapping
 203 Ω_{G_0} is bijective and linear, the rank vector \mathbf{r} of dimension $|E_0|$ is directly used as the code for this
 204 ingredient.

205 For the latter, we randomly embed \mathbf{P} into the space $[0, 1]^{|V|}$, a set of decimal number vectors, by
 206 a *random-key* trick [4], which is popularly used to solve the optimal sequencing tasks. For the
 207 details, the random-key representation encode a permutation with a vector of random numbers
 208 from $[0, 1]$, and the order of these random numbers reflects the permutation. For instance, the code
 209 $(0.46, 0.91, 0.33)$ would represent the permutation $2 \rightarrow 3 \rightarrow 1$, by which we naturally have its
 210 matrix form \mathbf{P} . Finally, the encoded strings are simply the concatenation of the two ingredients.

211 One advantage of the random-key trick is robustness to the structure of $\mathbb{H}_{G_0,R}$. Regardless of the
 212 irregularity of $\mathbb{H}_{G_0,R}$, we always have the regular key space $[0, 1]^{|V|}$, on which the operations such
 213 as addition and perturbation are always available. It implies that the proposed coding method is
 214 G_0 -independent, and many population-based methheuristics such as the one in [25] can be directly
 215 applied to graph-constrained structure search (see the numerical results given below.) .

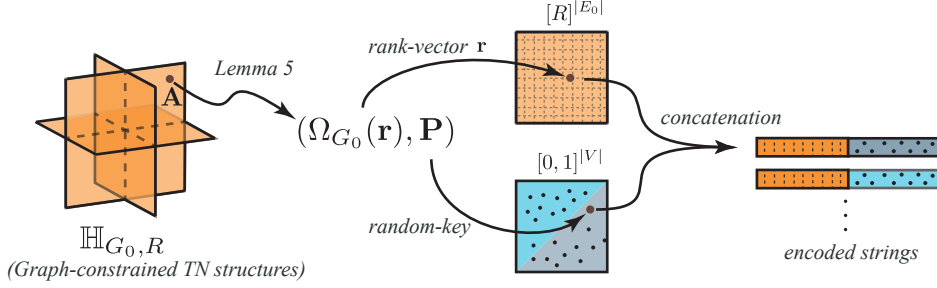


Figure 2: Illustration of encoding the graph-constrained TN structures into fixed-length strings. As Lemma 5, the structures are factorized by the rank-induced matrix $\Omega_{G_0}(\mathbf{r})$ and permutation matrix \mathbf{P} . In the method, $\Omega_{G_0}(\mathbf{r})$ is encoded by its non-zero entries, *i.e.* the rank-vector \mathbf{r} , into the space $[R]^{|E_0|}$ (the orange square). By the random-key trick, \mathbf{P} is represented a vector of random number in the “key space” typically $[0, 1]^{|V|}$ (the square with a mixed color in the figure). The final string is obtained by the concatenation of the two aspects. Note that, in the key space, different elements in the area with the same color represent the same permutation.

216 The proposed method gives more compact codes than the work in [25]. In the graph-constraint
 217 scenario, directly encoding the entries of the adjacency matrix as [25] cannot consider the “low-
 218 dimensional essence” of $\mathbb{H}_{G_0, R}$ due to the irregularity. However, by the proposed method, the
 219 code length is shorted as $\mathcal{O}(|V|)$ compared to $\mathcal{O}(|V|^2)$ in [25]. A shorter code length implies faster
 220 convergence and lower computational requirement for the population-based methods in general. For
 221 the proposed method, we also prove the coding efficiency given in the supplementary material, which
 222 reflects the gap of the code length from the Shannon entropy on $\mathbb{H}_{G_0, R}$.

223 4.2 Numerical results

224 In this section, we evaluate the practical effectiveness and efficiency of the proposed coding method
 225 on various benchmark tasks for tensor network representation (TNR).

226 4.2.1 Searching the optimal TN structures on synthetic data in TR format and beyond.

227 In this experiment, we examine whether using the proposed coding method can learn sufficiently
 228 good low-dimensional representation on synthetic tensors in TR (including TT) format.

229 **Data generation.** We generate batches of tensors with randomly selecting TR structures. Specifically,
 230 we first let the dimension of each tensor mode equal 3. Then, we randomly generate the TR-ranks
 231 at discrete uniform distribution on $\{1, 2, 3, 4\}$ and the cores at Gaussian distribution $N(0, 1)$, and
 232 randomly permute the tensor modes after contracting the cores.

233 **Experiment setup.** The proposed coding method are directly applied to the genetic algorithm (GA)
 234 in [25] by replacing its chromosome design aspect, where we let G_0 be a cycle graph and the rank
 235 bound R be equal to 7. Details of hyper-parameters on the GA are introduced in the supplementary
 236 material. For comparison, we also implement various types of TR decomposition methods with
 237 adaptive rank selection, which include the singular value decomposition (SVD) based method TR-
 238 SVD [47], least-squares-based method TR-ALSAR [47], Bayesian model Bayes-TR [35], and two
 239 general heuristics TR-LM [28] (exhaustive search) and TNGA [25] (population-based).

240 The experimental results are reported in Table 1, where the tensor order covers $\{4, 6, 8\}$ and the 5
 241 generated tensors for each order are denoted as **Trial A~E**. For performance evaluation, we use the
 242 *Eff.* index [25], the ratio of number of parameters between the learned structures and the ground-truth
 243 TRs, to illustrate the model efficiency. We also illustrate the relative square error (RSE) and the
 244 generation (Gen.) of the optimal individuals in TNGA and ours in the table.

245 **Results.** As shown in Table 1, only our method can always achieve the same or lower-dimensional
 246 representation than the ground-truth. We observe that most of the TR decomposition methods *fail*
 247 dealing with the permutation on tensor-modes, and such the fact would limit the application of
 248 the TR methods in the practical use on high-order problems. We also observe the performance of

Table 1: Experimental results of searching structures on synthetic data in TR format. In the table, *Eff.* denotes the parameter ratio between the structures by different methods and the ground-truths; *RSE* in round brackets indicates the relative square error (ignored if smaller than 10^{-4} .) and *Gen.* in angle brackets indicates the generation of the reported individual in TNGA and our method.

Order 4 – <i>Eff.</i> ↑ (<i>RSE</i> ↓) (<i>Gen.</i> ↓)						
Trial	TR-SVD [47]	TR-LM [28]	TR-ALSAR [47]	Bayes-TR [35]	TNGA [25]	Ours
A	1.00	1.00	0.21	1.00	1.00 ⟨004⟩	1.00 ⟨003⟩
B	0.64	1.00	1.00	0.64	1.00 ⟨002⟩	1.00 ⟨003⟩
C	1.17	1.17	0.23	1.00	1.17 ⟨005⟩	1.17 ⟨003⟩
D	0.57	0.57	0.32	1.25 (0.10)	1.00 ⟨003⟩	1.00 ⟨002⟩
E	0.43	0.48	0.40	0.40	1.00 ⟨007⟩	1.00 ⟨003⟩
Order 6 – <i>Eff.</i> ↑ (<i>RSE</i> ↓) (<i>Gen.</i> ↓)						
Trial	TR-SVD [47]	TR-LM [28]	TR-ALSAR [47]	Bayes-TR [35]	TNGA [25]	Ours
A	0.21	0.44	0.14 (2e-3)	0.25 (2e-3)	0.82 ⟨011⟩	1.00 ⟨010⟩
B	0.14	0.15	0.14	0.44 (0.40)	0.90 (6e-3) ⟨015⟩	1.00 ⟨009⟩
C	0.57	1.00	0.85	0.29	1.00 ⟨022⟩	1.00 ⟨012⟩
D	0.21	0.39	0.10	0.13	1.03 ⟨018⟩	1.16 ⟨010⟩
E	0.15	0.30	0.01 (0.02)	0.12	1.00 ⟨016⟩	1.00 ⟨007⟩
Order 8 – <i>Eff.</i> ↑ (<i>RSE</i> ↓) (<i>Gen.</i> ↓)						
Trial	TR-SVD [47]	TR-LM [28]	TR-ALSAR [47]	Bayes-TR [35]	TNGA [25]	Ours
A	0.10	0.16	0.03 (0.20)	0.03	0.48 ⟨017⟩	1.00 ⟨019⟩
B	0.09	0.43	0.06 (0.02)	0.06 (7e-4)	0.29 (2e-3) ⟨020⟩	1.02 ⟨015⟩
C	0.03	0.31	0.02 (0.01)	0.02	0.49 ⟨015⟩	1.11 ⟨025⟩
D	0.20	0.53	0.02 (0.07)	0.02 (0.02)	0.32 ⟨027⟩	1.06 ⟨013⟩
E	0.33	0.33	0.02 (0.02)	0.02 (3e-3)	0.23 ⟨023⟩	0.88 ⟨010⟩

Table 2: Experimental results of searching structures on synthetic data in various TN format. In the table, *Eff.* denotes the parameter ratio between the structures by different methods and the ground-truths; *RSE* in round brackets indicates the relative square error (ignored if smaller than 10^{-4} .) and *Gen.* in angle brackets indicates the generation of the reported individual of our methods. For rows, “ranks” means we fix the permutation part yet only learning the ranks, while “ranks+matching” means both the optimal ranks and permutation are learned.

TNs	Our method	Trial – <i>Eff.</i> ↑ (<i>RSE</i> ↓) (<i>Gen.</i> ↓)			
		A	B	C	D
T-Tree [42]	<i>ranks</i>	0.40 ⟨005⟩	0.41 (0.02) ⟨008⟩	0.40 (9e-3) ⟨006⟩	0.65 (0.04) ⟨005⟩
	<i>ranks+matching</i>	1.29 ⟨016⟩	1.17 ⟨014⟩	1.11 ⟨012⟩	1.55 ⟨012⟩
PEPS [38]	<i>ranks</i>	0.41 ⟨010⟩	0.43 (0.02) ⟨024⟩	0.39 (6e-3) ⟨027⟩	0.71 ⟨005⟩
	<i>ranks+matching</i>	1.14 ⟨013⟩	1.00 ⟨016⟩	1.00 ⟨007⟩	1.21 ⟨009⟩
H-Tucker [16]	<i>ranks</i>	0.49 (0.01) ⟨014⟩	0.64 ⟨010⟩	1.09 ⟨012⟩	0.81 ⟨006⟩
	<i>ranks+matching</i>	1.42 ⟨008⟩	1.21 ⟨023⟩	1.18 ⟨007⟩	1.29 ⟨011⟩
MERA [11, 33]	<i>ranks</i>	0.72 (0.01) ⟨012⟩	0.95 ⟨011⟩	1.93 ⟨011⟩	0.65 (0.04) ⟨014⟩
	<i>ranks+matching</i>	0.95 ⟨024⟩	1.32 ⟨008⟩	2.30 ⟨024⟩	1.00 ⟨027⟩

249 TNGA appears dramatically deterioration when increasing the tensor order. As analyzed at the end of
250 Section 4.1, TNGA suffers from the dimension explosion of the search space. In this case, TNGA
251 has to search the solution from about 4.6×10^{23} candidates, which is almost 8.0×10^{16} larger than
252 the one of ours.

253 **TN structure search not limit to TR.** The proposed coding method is also useful for many well-
254 known TNs in machine learning and physic not limit to TR. Under a similar setup for TR, we apply
255 the proposed method to the TNs including T-tree (order-7) [42], PEPS (order-6) [38], hieratical
256 Tucker (H-Tucker, order-6) [16] and multi-scale entanglement renormalization ansatz (MERA,

257 order-8) [11, 33]. Details of the data generation phase are given in the supplementary material.
 258 Table 2 illustrates the *Eff.*, *RSE* and *Gen.* values by our method, where the rows of “ranks” mean
 259 we only learn the optimal TN-ranks while the rows of “ranks+matching” mean both the ranks and
 260 permutation are learned by our method. As shown in Table 2, our method achieves the TN structures
 261 as good as or even better than the ground-truth for various TNs. In addition, we also observe that a
 262 correct permutation on modes would significantly improve the representational power of TNs.

263 4.2.2 Benchmarks on real-world data

264 We consider three benchmark TNR problem on real-world data, where two of them is to represent
 265 the data and the other one is to represent learning models. Details of the experiment setup and more
 266 results are given in the supplementary material.

- 267 1. **Image compression.** We use GA equipped with the proposed coding method (in TR format)
 268 to compress 14 natural images randomly chosen from BSD500 [1], where images are
 269 grayscale, resized by 256×256 , and tensorized into order-8 tensors by two different
 270 tensorization: a “Python-like” reshaping operation denoted by “Trivial” and visual data
 271 tensorization (VDT) [6, 24, 45], a image-resolution-based tensorization method. As the
 272 result, we show the compression ratio (CR, in log form) and RSE (in round brackets) by the
 273 methods TR-SVD, TR-LM and ours in Table 3, and visualize the summary statistics of the
 274 learned permutation by our method in Figure 3.
- 275 2. **Image completion.** The same method is also implemented on image completion, a task
 276 to predict missing pixels from the observation. In the experiment, 8 images from USC-
 277 SIPI [40] are chosen and tensorized by VDT of order-9. After that, the entries are randomly
 278 removed at uniform distribution under the missing rate $\{50\%, 70\%, 90\%\}$, respectively. We
 279 show the average of RSE of predicting the missing values in Table 4 compared with the
 280 TT/TR completion methods TT-SGD [45], TRLRF [44], TRALS [39].
- 281 3. **Reparameterization of tensorial Gaussian process (GP).** TNR is applied to parameteriz-
 282 ing the variational mean of GPs. In the experiment, we reparameterize the TT variational
 283 mean given in [20] by our method to search better structures. In a regression task on
 284 datasets CCPP [37], MG [14] and Protein [12], we have the TT variational mean of the
 285 order- $\{4, 6, 9\}$, respectively. In the result, we evaluate the performance by the number of
 286 parameters and mean square error (MSE, in the round brackets) shown in Table 5.

Table 3: Average of log compression ratio and RSE (in round brackets) for image decomposition.

	TR-SVD [47]	TR-LM [28]	Ours
Trivial	0.95(0.14)	0.94(0.14)	1.35(0.14)
VDT	1.11(0.15)	1.07(0.14)	1.30(0.14)

Table 4: Average of RSE on image completion under various missing percentage.

	TTSGD [45]	TRLRF [44]	TRALS [39]	Ours
50%	0.16	0.12	0.13	0.11
70%	0.17	0.13	0.13	0.12
90%	0.18	0.20	0.18	0.16

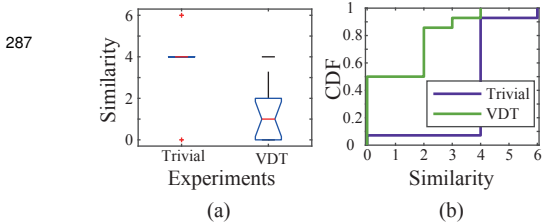


Figure 3: Visualization of statistics on the similarity to the original permutation.

288 **VDT is verified as a more effective way for tensorization.** The results in Table 3 show that,
 289 our method owns higher compression ratio under close RSE compared to other methods. More
 290 importantly, the results show a significant difference when learning structures from two tensorization.
 291 Figure 3 illustrates the statistics on the similarity between the original permutation and the learned
 292 ones by our method. We observe from Figure 3(a) that in VDT the learned permutation is *significantly*
 293 closer to the original one than that in the “Trivial”. Additionally, Figure 3(b) shows the cumulative
 294 distribution function (CDF), where we can see that, in VDT the probability is larger than 0.8 for
 295

Table 5: Number of parameters and MSE (in round brackets) of GP regression under three datasets.

	CCPP	MG	Protein
TTGP [20]	2640 (0.06)	3360 (0.33)	2880 (0.74)
Ours	2244 (0.06)	3008 (0.33)	2032 (0.74)

296 the similarity being smaller than or equal to 2 . It implies that with a large probability the learned
297 structures in VDT own at most a pair of permutation difference compared to the original one. On the
298 contrary, for “Trivial” the probability is almost zero in the same interval. Hence, it is verified from
299 the empirical results by our method that VDT is more effective way for image tensorization than the
300 trivially reshaping operations.

301 **Exploring TN structures obtains lower-dimensional representation from incomplete data.** As
302 shown in Table 4, our method achieve a comparable performance on the image completion task.
303 Especially when the missing ratio is high, our method is forced to explore better TN structures not
304 limit to the ranks, such that the lower-dimensional representation would be applied and results in
305 more accurate prediction. Similar claims were also discussed in recent works [7, 17].

306 **Tensor-reparameterization: a potential way to compress learning models.** TNs are known as
307 an efficient framework to compress learnables variables by low-dimensional cores. In the experi-
308 ment, we illustrate from a “proof-of-concept” level that the model would be further compressed by
309 *re*-parameterizing the learned TN in model. As shown in Table 5, we always use fewer parameters
310 than its “teacher” model TTGP [20] to achieve the same MSE on the three datasets. It implies that
311 our method give more efficient TNR by search better structures. Unlike training the model with
312 simultaneously searching TN structures, we empirically find that searching better structures from the
313 well-trained model in TN format would achieve better compression ratio. We intuitively conjecture
314 that, by structure search, it is likely to obtain more efficient representation for a tensor, which has
315 been in low-rank TN format. In the training phase, on the other hand, the models are not significantly
316 low-rank in general. Therefore, the tensor reparameterization often gives better performance in
317 practice. A rigorous analysis on this issue is still an open problem.

318 5 Discussion

319 Our experiments show good TN structures including ranks and permutations can be effectively learned
320 in practice by the proposed coding method under extensive family of graph constraints, and our
321 theoretical results show the the superior performance is thanks to the low-dimensional essence hidden
322 behind the irregularity of the graph-constrained TN structures. More surprisingly, Proposition 9
323 shows that such the low-dimensional essence of TN structures is ubiquitous for most of practical
324 TNs. As a consequence, we expect this work can promote the understanding on the structure search
325 issue on tensor networks from both the theoretical and practical aspects, and the empirical claims in
326 experiments are also expected to inspire more potential applications of TNs in machine learning.

327 **Limitation.** Theoretically, we only study the TNs, which do not contain the internal cores. Some
328 well-known models like (H-)Tucker and MERA are not contained in the theory, although the proposed
329 coding method works well for those models in experiments. Empirically, the proposed coding method
330 is more suitable for the population-based methods like GAs, which are still computationally expensive
331 compared to other heuristics. Also, the experiments on real-world benchmarks are only illustrative
332 and proof-of-concept. More numerical results are necessary if stronger statements such as the
333 performance improvement are expected.

334 6 Related works

335 Learning the optimal TN structures is a generalization of the rank selection issue for TN models [8, 9,
336 18, 26–28, 34, 43, 46, 47], and it is known as a tough task especially for the models that contain cycles
337 in the topology [3, 23, 42]. More recently, there are several studies on learning TN structures [17, 19,
338 21, 25] in a more general form. Another line of works that are close to ours are studies focusing on
339 the partition issue for H-Tucker decomposition [2, 13, 15], where the modes would be clustered to
340 determine the optimal tree structure. Unlike them, this work is the first to solve the optimal matching
341 problem as illustrated in Figure. 1. Moreover, we are the only few to theoretically study the structure
342 search issue for tensor networks. From the algorithmic aspect, the random-key trick in our coding
343 method is first proposed by [4], and popularly applied to solving difficult sequencing tasks such as
344 the “travelling salesman problem” and the “clique problem” [31] in computational graph theory. Our
345 method is also close to the subgraph search issue in the recent work [41], yet we focus on the different
346 tasks and issues.

347 **References**

- 348 [1] Pablo Arbelaez, Michael Maire, Charless Fowlkes, and Jitendra Malik. Contour detection
349 and hierarchical image segmentation. *IEEE transactions on pattern analysis and machine*
350 *intelligence*, 33(5):898–916, 2010.
- 351 [2] Jonas Ballani and Lars Grasedyck. Tree adaptive approximation in the hierarchical tensor
352 format. *SIAM journal on scientific computing*, 36(4):A1415–A1431, 2014.
- 353 [3] Kim Batselier. The trouble with tensor ring decompositions. *arXiv preprint arXiv:1811.03813*,
354 2018.
- 355 [4] James C Bean. Genetic algorithms and random keys for sequencing and optimization. *ORSA*
356 *journal on computing*, 6(2):154–160, 1994.
- 357 [5] Lowell W Beineke, Robin J Wilson, Peter J Cameron, et al. *Topics in algebraic graph theory*,
358 volume 102. Cambridge University Press, 2004.
- 359 [6] Johann A Bengua, Ho N Phien, Hoang Duong Tuan, and Minh N Do. Efficient tensor completion
360 for color image and video recovery: Low-rank tensor train. *IEEE Transactions on Image*
361 *Processing*, 26(5):2466–2479, 2017.
- 362 [7] Yunfeng Cai and Ping Li. Tensor completion via tensor networks with a tucker wrapper. *arXiv*
363 *preprint arXiv:2010.15819*, 2020.
- 364 [8] Yunfeng Cai and Ping Li. A blind block term decomposition of high order tensors. 2021.
- 365 [9] Zhiyu Cheng, Baopu Li, Yanwen Fan, and Yingze Bao. A novel rank selection scheme in tensor
366 ring decomposition based on reinforcement learning for deep neural networks. In *ICASSP 2020-*
367 *2020 IEEE International Conference on Acoustics, Speech and Signal Processing (ICASSP)*,
368 pages 3292–3296. IEEE, 2020.
- 369 [10] Andrzej Cichocki, Anh-Huy Phan, Qibin Zhao, Namgil Lee, Ivan Oseledets, Masashi Sugiyama,
370 Danilo P Mandic, et al. Tensor networks for dimensionality reduction and large-scale opti-
371 mization: Part 2 applications and future perspectives. *Foundations and Trends® in Machine*
372 *Learning*, 9(6):431–673, 2017.
- 373 [11] Lukasz Cincio, Jacek Dziarmaga, and Marek M Rams. Multiscale entanglement renormalization
374 ansatz in two dimensions: quantum ising model. *Physical Review Letters*, 100(24):240603,
375 2008.
- 376 [12] Dheeru Dua and Casey Graff. UCI machine learning repository, 2017.
- 377 [13] Antonio Falcó, Wolfgang Hackbusch Nouy, et al. Geometry of tree-based tensor formats in
378 tensor banach spaces. *arXiv preprint arXiv:2011.08466*, 2020.
- 379 [14] Gary William Flake and Steve Lawrence. Efficient svm regression training with smo. *Machine*
380 *Learning*, 46(1):271–290, 2002.
- 381 [15] Cécile Haberstich, Anthony Nouy, and Guillaume Perrin. Active learning of tree tensor networks
382 using optimal least-squares. *arXiv preprint arXiv:2104.13436*, 2021.
- 383 [16] Wolfgang Hackbusch and Stefan Kühn. A new scheme for the tensor representation. *Journal of*
384 *Fourier analysis and applications*, 15(5):706–722, 2009.
- 385 [17] Meraj Hashemizadeh, Michelle Liu, Jacob Miller, and Guillaume Rabusseau. Adaptive tensor
386 learning with tensor networks. *arXiv preprint arXiv:2008.05437*, 2020.
- 387 [18] Cole Hawkins and Zheng Zhang. Bayesian tensorized neural networks with automatic rank
388 selection. *arXiv preprint arXiv:1905.10478*, 2019.
- 389 [19] Kohei Hayashi, Taiki Yamaguchi, Yohei Sugawara, and Shin-ichi Maeda. Exploring unexplored
390 tensor network decompositions for convolutional neural networks. In *Advances in Neural*
391 *Information Processing Systems*, pages 5553–5563, 2019.

- 392 [20] Pavel Izmailov, Alexander Novikov, and Dmitry Kropotov. Scalable gaussian processes with
393 billions of inducing inputs via tensor train decomposition. In *International Conference on*
394 *Artificial Intelligence and Statistics*, pages 726–735. PMLR, 2018.
- 395 [21] Maxim Kodryan, Dmitry Kropotov, and Dmitry Vetrov. Mars: Masked automatic ranks selection
396 in tensor decompositions. *arXiv preprint arXiv:2006.10859*, 2020.
- 397 [22] I Krasikov, A Lev, and BD Thatte. Upper bounds on the automorphism group of a graph.
398 *Discrete Math.*, 256(math. CO/0609425):489–493, 2006.
- 399 [23] Joseph M Landsberg, Yang Qi, and Ke Ye. On the geometry of tensor network states. *arXiv*
400 *preprint arXiv:1105.4449*, 2011.
- 401 [24] Jose I Latorre. Image compression and entanglement. *arXiv preprint quant-ph/0510031*, 2005.
- 402 [25] Chao Li and Zhun Sun. Evolutionary topology search for tensor network decomposition. In
403 *Proceedings of the 37th International Conference on Machine Learning (ICML)*, 2020.
- 404 [26] Nannan Li, Yu Pan, Yaran Chen, Zixiang Ding, Dongbin Zhao, and Zenglin Xu. Heuristic rank
405 selection with progressively searching tensor ring network. *Complex & Intelligent Systems*,
406 pages 1–15, 2021.
- 407 [27] Zhen Long, Ce Zhu, Jiani Liu, and Yipeng Liu. Bayesian low rank tensor ring model for image
408 completion. *arXiv preprint arXiv:2007.01055*, 2020.
- 409 [28] Oscar Mickelin and Sertac Karaman. On algorithms for and computing with the tensor ring
410 decomposition. *Numerical Linear Algebra with Applications*, 27(3):e2289, 2020.
- 411 [29] Román Orús. A practical introduction to tensor networks: Matrix product states and projected
412 entangled pair states. *Annals of Physics*, 349:117–158, 2014.
- 413 [30] Ivan V Oseledets. Tensor-train decomposition. *SIAM Journal on Scientific Computing*,
414 33(5):2295–2317, 2011.
- 415 [31] Panos M Pardalos and Jue Xue. The maximum clique problem. *Journal of global Optimization*,
416 4(3):301–328, 1994.
- 417 [32] Karl Pearson. Historical note on the origin of the normal curve of errors. *Biometrika*, pages
418 402–404, 1924.
- 419 [33] Justin Reyes and Miles Stoudenmire. A multi-scale tensor network architecture for classification
420 and regression. *arXiv preprint arXiv:2001.08286*, 2020.
- 421 [34] Farnaz Sedighin, Andrzej Cichocki, and Anh-Huy Phan. Adaptive rank selection for tensor ring
422 decomposition. *IEEE Journal of Selected Topics in Signal Processing*, 15(3):454–463, 2021.
- 423 [35] Zerui Tao and Qibin Zhao. Bayesian tensor ring decomposition for low rank tensor completion.
424 In *International Workshop on Tensor Network Representations in Machine Learning, IJCAI*,
425 2020.
- 426 [36] Ledyard R Tucker. Some mathematical notes on three-mode factor analysis. *Psychometrika*,
427 31(3):279–311, 1966.
- 428 [37] Pınar Tüfekci. Prediction of full load electrical power output of a base load operated combined
429 cycle power plant using machine learning methods. *International Journal of Electrical Power*
430 *& Energy Systems*, 60:126–140, 2014.
- 431 [38] Frank Verstraete and J Ignacio Cirac. Renormalization algorithms for quantum-many body
432 systems in two and higher dimensions. *arXiv preprint cond-mat/0407066*, 2004.
- 433 [39] Wenqi Wang, Vaneet Aggarwal, and Shuchin Aeron. Efficient low rank tensor ring completion.
434 In *Proceedings of the IEEE International Conference on Computer Vision*, pages 5697–5705,
435 2017.
- 436 [40] Allan G Weber. The usc-sipi image database version 5. *USC-SIPI Report*, 315(1), 1997.

- 437 [41] Hansi Yang, Quanming Yao, and James Kwok. Tensorizing subgraph search in the supernet.
438 *arXiv preprint arXiv:2101.01078*, 2021.
- 439 [42] Ke Ye and Lek-Heng Lim. Tensor network ranks. *arXiv preprint arXiv:1801.02662*, 2019.
- 440 [43] Tatsuya Yokota, Qibin Zhao, and Andrzej Cichocki. Smooth parafac decomposition for tensor
441 completion. *IEEE Transactions on Signal Processing*, 64(20):5423–5436, 2016.
- 442 [44] Longhao Yuan, Chao Li, Danilo Mandic, Jianting Cao, and Qibin Zhao. Tensor ring decomposi-
443 tion with rank minimization on latent space: An efficient approach for tensor completion. In
444 *Proceedings of the AAAI Conference on Artificial Intelligence*, volume 33, pages 9151–9158,
445 2019.
- 446 [45] Longhao Yuan, Qibin Zhao, Lihua Gui, and Jianting Cao. High-order tensor completion via
447 gradient-based optimization under tensor train format. *Signal Processing: Image Communica-*
448 *tion*, 73:53–61, 2019.
- 449 [46] Qibin Zhao, Liqing Zhang, and Andrzej Cichocki. Bayesian cp factorization of incomplete
450 tensors with automatic rank determination. *IEEE transactions on pattern analysis and machine*
451 *intelligence*, 37(9):1751–1763, 2015.
- 452 [47] Qibin Zhao, Guoxu Zhou, Shengli Xie, Liqing Zhang, and Andrzej Cichocki. Tensor ring
453 decomposition. *arXiv preprint arXiv:1606.05535*, 2016.
- 454 [48] Yu-Bang Zheng, Ting-Zhu Huang, Xi-Le Zhao, Qibin Zhao, and Tai-Xiang Jiang. Fully-
455 connected tensor network decomposition and its application to higher-order tensor completion.
456 2021.

457 **Checklist**

- 458 1. For all authors...
- 459 (a) Do the main claims made in the abstract and introduction accurately reflect the paper's
460 contributions and scope? [Yes]
- 461 (b) Did you describe the limitations of your work? [Yes] See Section 5
- 462 (c) Did you discuss any potential negative societal impacts of your work? [N/A]
- 463 (d) Have you read the ethics review guidelines and ensured that your paper conforms to
464 them? [Yes]
- 465 2. If you are including theoretical results...
- 466 (a) Did you state the full set of assumptions of all theoretical results? [Yes]
- 467 (b) Did you include complete proofs of all theoretical results? [Yes] All proofs are given
468 in the supplementary material.
- 469 3. If you ran experiments...
- 470 (a) Did you include the code, data, and instructions needed to reproduce the main exper-
471 imental results (either in the supplemental material or as a URL)? [Yes] Codes with
472 illustrative experiments is uploaded
- 473 (b) Did you specify all the training details (e.g., data splits, hyperparameters, how they
474 were chosen)? [Yes] See the supplementary material.
- 475 (c) Did you report error bars (e.g., with respect to the random seed after running experi-
476 ments multiple times)? [No] Yet we show the results for each sample such as images
477 or synthetic data in the supplementary material. The error bars can be estimated from
478 those results.
- 479 (d) Did you include the total amount of compute and the type of resources used (e.g., type
480 of GPUs, internal cluster, or cloud provider)? [Yes] See the supplementary material.
- 481 4. If you are using existing assets (e.g., code, data, models) or curating/releasing new assets...
- 482 (a) If your work uses existing assets, did you cite the creators? [N/A]
- 483 (b) Did you mention the license of the assets? [N/A]
- 484 (c) Did you include any new assets either in the supplemental material or as a URL? [N/A]
- 485
- 486 (d) Did you discuss whether and how consent was obtained from people whose data you're
487 using/curating? [N/A]
- 488 (e) Did you discuss whether the data you are using/curating contains personally identifiable
489 information or offensive content? [N/A]
- 490 5. If you used crowdsourcing or conducted research with human subjects...
- 491 (a) Did you include the full text of instructions given to participants and screenshots, if
492 applicable? [N/A]
- 493 (b) Did you describe any potential participant risks, with links to Institutional Review
494 Board (IRB) approvals, if applicable? [N/A]
- 495 (c) Did you include the estimated hourly wage paid to participants and the total amount
496 spent on participant compensation? [N/A]